

Title:

Using the IUCN Red List to map threats to terrestrial vertebrates at global scale

Author list:

Michael B. J. Harfoot^{1*}, Alison Johnston^{2,3}, Andrew Balmford³, Neil D. Burgess^{1,4,3}, Stuart H. M. Butchart^{5,3}, Maria P. Dias^{5,6}, Carolina Hazin⁵, Craig Hilton-Taylor⁷, Michael Hoffmann⁸, Nick J. B. Isaac⁹, Lars L. Iversen^{4,10}, Charlotte L. Outhwaite¹¹, Piero Visconti¹², Jonas Geldmann^{3,4*}

Affiliation:

¹ UN Environment Programme World Conservation Monitoring Centre (UNEP-WCMC), 219 Huntingdon Road, Cambridge, CB3 0DL, United Kingdom

² Cornell Lab of Ornithology, 159 Sapsucker Woods Road, Ithaca, NY 14850 USA

³ Conservation Science Group, Department of Zoology, University of Cambridge, Downing St., Cambridge CB2 3EJ, United Kingdom

⁴ Center for Macroecology, Evolution and Climate, Globe Institute, University of Copenhagen, Universitetsparken 15, DK-2100, Copenhagen E, Denmark

⁵ BirdLife International, The David Attenborough Building, Pembroke Street Cambridge CB2 3QZ, United Kingdom

⁶ MARE – Marine and Environmental Sciences Center, ISPA – Instituto Universitário, Lisboa, Portugal

⁷ IUCN, The David Attenborough Building, Pembroke Street Cambridge CB2 3QZ, United Kingdom

⁸ Conservation and Policy, Zoological Society of London, Regent's Park, London, NW1 4RY

⁹ UK Centre for Ecology & Hydrology, Maclean Building, Crowmarsh Gifford, Wallingford, OX10 8BB

¹⁰ Department of Environmental Science, Policy, and Management, University of California, Berkeley, CA 94720

¹¹ Centre for Biodiversity and Environment Research, University College London, Gower Street, London, WC1E 6BT, United Kingdom

¹² IIASA - International Institute for Applied Systems Analysis Schlossplatz 1, A-2361 Laxenburg, Austria

* Corresponding authors: Jonas Geldmann: jgeldmann@sund.ku.dk and Michael B. J. Harfoot: mike.harfoot@unep-wcmc.org

Keywords: threat; biodiversity; hunting; logging; agriculture; IUCN Red List;

Abstract

The Anthropocene is characterized by unparalleled human impact on other species, potentially ushering in the sixth mass extinction. Yet mitigation efforts remain hampered by limited information on the spatial patterns and intensity of the threats driving global biodiversity loss. Here we use expert-derived information from the IUCN Red List on threats to 23,271 species, representing all terrestrial amphibians, birds and mammals, to generate global maps of the six major threats to these groups: agriculture, hunting & trapping, logging, pollution, invasive species, and climate change. Our results show that agriculture and logging are pervasive in the tropics, and that hunting & trapping is the most geographically widespread threat to mammals and birds. Additionally, current representations of human pressure underestimate overall pressure

42 on biodiversity, due to the exclusion of threats like hunting and climate change. Alarminglly, this is
43 particularly the case in areas of the highest biodiversity importance.

Main text

The world has entered the Anthropocene, characterized by unparalleled human impact on the global environment^{1,2}, and associated with devastating biodiversity losses^{3,4}. Despite this, we still have limited information about the spatial patterns and intensity of the threats responsible for this crisis^{5,6}. This is particularly true for pressures such as over-exploitation, pollution, and invasive species, for which no suitable remotely sensed proxies exist⁷⁻⁹. Additionally, for threats where remotely sensed data are available, these measure physical processes such as habitat conversion or the expansion of infrastructure¹⁰⁻¹². However, the specific impact on species and habitats does not necessarily scale with the intensity of the processes but is highly context specific¹³. As a result, existing representations of pressures may not adequately capture impacts on ecosystems and species, and lack the detail required to target conservation actions efficiently^{14,15}. Better information on the spatial intensity of threats and how they affect species on the ground is critically important for improving conservation responses⁵.

The IUCN Red List of Threatened Species™ (hereafter ‘Red List’) is one of the richest and most authoritative data-sources in conservation¹⁶ derived from tens of thousands of hours from expert volunteer contributors worldwide¹⁷. To date, over 100,000 species have been assessed against the IUCN Red List Categories and Criteria, including all amphibians, birds and mammals¹⁸. For assessed species, experts have evaluated the threats affecting individual species using a standardized method and classification scheme¹⁹. However, information on the spatial occurrence of threats affecting a given species within its distribution is not collected systematically and is limited to documenting whether the species is affected by a given threat anywhere within its range. Additionally, there are no comprehensive spatial summaries of these threats to species.

Here we address these knowledge gaps through a novel approach to develop global maps for the six main threats affecting terrestrial amphibians, birds, and mammals (23,271 species in total assessed by the IUCN Red List): 1) agriculture, 2) hunting & trapping, 3) logging, 4) pollution, 5) invasive species (including pathogens such as chytrid), and 6) climate change⁴. To generate these maps, we utilize data from the thousands of species assessed in the Red List in a probabilistic framework which explicitly incorporates the spatial uncertainty introduced by only knowing that a species is affected somewhere in the range. Our approach is inspired by methods from citizen science, which face similar issues resulting from large quantities of data with unknown and varying precision of the individual observations. We first used a set of simulated threat maps, with the same properties as the Red List, to develop our model framework and assess different model-parameterizations ability to reproduce our simulated threat data (Extended Data Figure 1). Choosing the model which showed the highest concordance with the simulated data (Extended Data Figure 2), we then mapped the impact probability of each of the six threats using the actual Red List data. Following this, we then evaluated the predictions of the best-fit model against two independent data sources; one on

threats assessed by experts within ca. 6,000 Key Biodiversity Areas (KBAs)²⁰ and a dataset based on remotely sensed forest-change¹⁰. Both evaluations showed that our predictions were consistent with empirical data (Fig. S5-11), giving us confidence in the validity of our approach to map the impact of threats at a global scale.

Results and discussion

Major threats across taxa and space

Our method estimates the ‘impact probability’, which is the probability that a randomly selected species occurring in a given grid-cell is impacted in that cell by a particular threat, while accounting for the spatial uncertainty inherent in the Red List data. Across the six threats, amphibians had higher average impact probabilities (median threat probability across cells, $M = 0.11$; 95% interval, $I_{95\%} = 7 \times 10^{-3}$ -0.42) followed by mammals ($M = 0.10$; $I_{95\%} = 0.04$ -0.21) and birds ($M = 0.05$; $I_{95\%} = 0.01$ -0.19). This accords with the higher overall extinction risk of amphibians²¹. The largest uncertainties in the estimated impact probabilities were observed in the Congo Basin for amphibians, and across the Sahara and Central Asia for birds and mammals (Figs. 1h; 2h; 3h). For amphibians, agriculture was the most prevalent of any threat, having the highest probability of impact in 44% of the mapped area (Fig. 1g), while hunting & trapping was the most prevalent threat for birds (in 50% of mapped range; Fig. 2g) and overwhelmingly for mammals (73% of mapped range; Fig. 3g). Our findings support existing non-spatial assessments⁵ and policy syntheses⁴. There are sizeable continental areas in which there was greater than 50% chance that any given amphibian, mammal or bird species was threatened by logging, hunting & trapping, agriculture, invasive species or climate change (between 1.6-10.8 million km²; Extended Data Figure 3).

Southeast Asia, particularly the islands of Sumatra and Borneo, as well as Madagascar, exhibited high probability of impact across all threats and all taxa (Fig. 1-3). For amphibians, Europe stood out as a region with high impact probabilities, driven by a combination of agriculture, invasive species (typically chytrid fungus), and pollution (Fig. 1), while polar regions, the east coast of Australia and South Africa showed the highest impact probabilities for climate change, driven in particular by impacts on birds (Fig. 2). For mammals and birds, high probabilities of species being impacted by hunting & trapping were found across much of the terrestrial surface (Fig. 2, 3).

Across all taxa, agriculture, followed by hunting & trapping, and logging had the highest average impact probability (Extended Data Figure 3), while the probability of being impacted by pollution was low in most parts of the terrestrial world. The probability of a species being impacted by invasive species was on average low for amphibians ($M = 0.01$, $I_{95\%} = 2.3 \times 10^{-10}$ -0.65), mammals ($M = 0.05$, $I_{95\%} = 1.7 \times 10^{-9}$ -0.21), and birds ($M = 0.04$, $I_{95\%} = 8.4 \times 10^{-11}$ -0.13). However, this probability of impact was elevated in some locations for birds and amphibians. For birds, the higher probabilities were seen on those islands included in our models.

For amphibians they were located on the east coast of Australia, the dry forests of Madagascar, Europe and North America, the latter being consistent with observational data of recorded chytrid outbreaks²².

Our approach is also able to highlight where knowledge gaps about species distributions and threats most influence the certainty of our predictions by including the proportion of Data Deficient species in our analyses. While not a perfect proxy for knowledge-certainty, the proportion of Data Deficient species is likely to correlate with overall certainty in knowledge in a given region. Thus, it is reasonable to assume that if particular regions are less well studied there will also be less certainty about the distribution, conservation status, and threats to species in that region. We show the largest uncertainties in the estimated impact probabilities were observed in the Congo Basin for amphibians, and across the Sahara and Central Asia for birds and mammals (Fig. 1h; 2h; 3h). These regions have previously been identified as data-poor²³ and increased sampling would likely both improve our model predictions and improve our understanding of threats to species in these areas.

Priorities for threat mitigation

To identify areas of priority for threat mitigation, it is necessary to combine the estimates of the probability that a threat impact occurs with information on spatial pattern of biodiversity importance. We therefore developed ‘conservation risk maps’ for each threat by multiplying our ‘probability of impact’ with species richness (Extended Data Figures 4 - 6). For each threat and taxonomic group in turn we then identified hotspot areas as the top decile (Fig. 4). Given the resolution of the Red List data and that of our maps (50 x 50 km), the latter are not intended for guiding local conservation action, but illustrate overall patterns of conservation priorities for mitigating threats to biodiversity across Earth.

Hotspots of highest risk from agriculture, hunting & trapping, and logging were primarily located in the tropics. Conversely, hotspots of risk from pollution were found in Europe, driven by impacts on amphibians and mammals (Fig. 4a-f). Except for the Australian East coast, invasive species risk hotspots showed distinct patterns for the three taxa. Amphibians and mammals were particularly threatened in different parts of the New World and Europe, while hotspots of risk for birds were found on islands, consistent with existing syntheses^{7,8,24}, distributed along coastal areas, and across eastern and southern Africa.

Hotspots of risk for different taxa rarely overlapped, and overall, 50% of the terrestrial surface was identified as a hotspot of risk from at least one threat for one taxonomic group (Fig. 4g). High priority areas for threat mitigation were identified as: The Himalayas, Southeast Asia, the east coast of Australia, the dry forest of Madagascar, the Albertine Rift and Eastern Arc Mountains in Eastern Africa, the Guinean forests of West Africa, Atlantic Forest, the Amazon basin and the Northern Andes into Panama and Costa Rica in South and Central America (Fig 4g).

Augmenting existing threat maps

Existing global threat maps estimate the extent of pressures or changes to the natural world such as land-use, human settlements, and infrastructure^{11,12,25}. These capture the intensity of some of the most important human pressures on the environment, but they do not measure how these drivers and processes affect species and habitats¹³ and do not include all of the most important threats to biodiversity^{5,26,27}. Our method, based on Red List data on threats to thousands of species, provides valuable complementary information. To assess the difference between maps based on drivers and processes and maps based on impacts on species, we compared our maps of impact probability with the latest version of the Human Footprint¹¹.

We first created a new composite land-use impact probability layer as the mean of agriculture and logging for each pixel, to better compare with the land-use component of the Human Footprint. We found a weak positive relationship between our measure of probability of impact from land-use and the Human Footprint (Fig. 5a). However, there were discrepancies, with the Human Footprint generally showing a lower pressure from land use in wilderness areas and higher pressures in urbanised areas compared with our impact probability map (Fig. 5d). This divergence was even more pronounced for hunting & trapping, with Human Footprint values relatively low across most of the tropical forests, where our maps suggest high impact from hunting & trapping (Fig. 5b,e). The largest discrepancy was with climate change, for which some areas, especially in the Arctic, show a low Human Footprint but high impacts from climate change (Fig. 5c,f). Our results indicate that current global descriptions of pressure potentially underestimate the impact of human threats to biodiversity, particularly in the most pristine areas that are likely to be of high importance for nature conservation²⁸⁻³⁰. However, given the constraints associated with the species based threat assessment used in the Red List, it is also plausible that our approach could overestimate the probability of impact for areas which, in reality, have low levels of threat and might serve as refugia for species. Thus, our findings suggest that multiple approaches are needed, traversing drivers, processes and effects to better understand the multifaceted nature of human pressures on biodiversity. Additionally, while our threat maps represent the impacts on extant species to threats from human drivers, they omit impacts from pressures that have already led to extirpations or extinctions. For example, in Europe where a large part of the original fauna has already been lost³¹, maps of accumulated drivers, such as the Human Footprint, might better represent the true extent of human impacts than the response of the remaining species to current threatening factors³².

Filling important knowledge-gaps

Our approach helps to address important data- and knowledge-gaps in more direct measures of threats based on field assessments by using a globally consistent, robust, and high-quality dataset^{16,33,34}. For hunting & trapping, pollution, and invasive species, all of which are implicated in dramatic population declines of native species around the world^{7,35-37}, our approach provides a novel and in some instances the only way of mapping their impacts on biodiversity at regional to global scales⁹. Even for threats where remotely sensed

maps of human activity exist (e.g. agriculture and forest loss), our maps add additional information on where species appear to be adversely impacted by these activities. Regional analyses have also included information about species distributions to account for where threats are likely to affect most individuals³⁸, but while valuable, such analyses still assume that threats are uniformly likely across the species range. Our results show that patterns of impact often differ from patterns of occurrence of threatening processes or the number of species affected by a given threat³⁹. This discrepancy in part relates to current threat representations omitting some types of threats (e.g. 'empty forest syndrome' resulting from pervasive hunting and trapping in apparently pristine forest^{6,40,41}). Additionally, the effect of a threat varies with the specific context, so that the same intensity of a threatening process can have different impact in different places or on different species. For example, forest loss affects a larger proportion of species in Southeast Asia, where little primary forest is left compared with the Amazon, where substantial forest remains despite high rates of loss in both places¹⁰.

Our analysis and maps do not cover any plant or invertebrate groups, many of which are severely impacted by multiple threats⁴²⁻⁴⁴ and whose hotspots of diversity and conservation importance are not always overlapping with those of terrestrial vertebrates⁴⁵ and also is limited in terms of its representation of freshwater taxa. Additionally, our threat representation estimates the probability of a random species in a given location being affected by a threat. While we believe this is closer to measuring the impact than mapping the drivers of threats, it does not capture the severity of the impact⁴⁶. Thus, while our maps show that invasive alien species are not affecting very large numbers of species overall, the native species affected are often undergoing rapid population declines as a consequence^{8,47,48}, particularly on many oceanic islands^{7,8,24}. We acknowledge that it is possible that expert predispositions may influence assessments of some threats to some species on the Red List. However, the Red List assessment process is explicitly designed to mitigate this risk, by ensuring that assessments are grounded in evidence from peer-reviewed and other vetted sources, properly documented, applied in a consistent fashion and subjected to independent review (see SI for a full description of the Red List assessment process).

Improving future threat mapping

The current biodiversity crisis derives from current levels of action and resources being insufficient or misaligned to mitigate and reverse the increase in human pressures on the environment^{3,49}. Thus, while the ultimate objective of conservation is to preserve biodiversity, understanding and addressing threats to nature is essential to ensure action is targeted at the places most in need. Our maps provide an important step towards a more complete understanding of the distribution and impact of threats. However, this does not suggest that these maps cannot be improved. Indeed, a key strength of our approach is that it demonstrates a new way forward. The maps can help to stimulate and inform models of how biodiversity is currently being impacted by a broader range of human activities than is typically considered. They can also help

inform future Red Listing assessments, by providing a more systematic understanding of potential threats within the range of focal species. Additionally, other sources of data on anthropogenic pressures to biodiversity, such as from acoustic monitoring, camera-traps, drones, and satellite imagery, will be critical to help augment and improve our maps and develop more robust statistical synthesis of the impact of threats to biodiversity. There is substantial potential for these maps to drive conservation science, and policy. However, given the resolution of the maps and the precision of the underlying data we caution against using these maps to guide local conservation action. Their value is in illuminating global patterns and demonstrating a new approach to mapping threat impacts as well as to inform decisions within the context of international policy processes such as the Convention on Biological Diversity and Sustainable Development Goals, recognizing that understanding where in the world different threats impact terrestrial vertebrate species is essential for designing effective conservation responses¹⁵.

References

- 1 Steffen, W., Grinevald, J., Crutzen, P. & McNeill, J. The Anthropocene: conceptual and historical perspectives. *Philosophical Transactions of the Royal Society a-Mathematical Physical and Engineering Sciences* **369**, 842-867, doi:10.1098/rsta.2010.0327 (2011).
- 2 Barnosky, A. D. *et al.* Has the Earth's sixth mass extinction already arrived? *Nature* **471**, 51-57 (2011).
- 3 Tittensor, D. P. *et al.* A mid-term analysis of progress toward international biodiversity targets. *Science* **346**, 241-244, doi:10.1126/science.1257484 (2014).
- 4 IPBES. Summary for policymakers of the global assessment report on biodiversity and ecosystem services of the Intergovernmental Science-Policy Platform on Biodiversity and Ecosystem Services. 39 (Intergovernmental Science-Policy Platform on Biodiversity and Ecosystem Services, 2019).
- 5 Joppa, L. N. *et al.* Filling in biodiversity threat gaps. *Science* **352**, 416-418, doi:10.1126/science.aaf3565 (2016).
- 6 Benítez-López, A., Santini, L., Schipper, A. M., Busana, M. & Huijbregts, M. A. J. Intact but empty forests? Patterns of hunting-induced mammal defaunation in the tropics. *PLOS Biology* **17**, e3000247, doi:10.1371/journal.pbio.3000247 (2019).
- 7 Early, R. *et al.* Global threats from invasive alien species in the twenty-first century and national response capacities. *Nature Communications* **7**, 12485, doi:10.1038/ncomms12485 (2016).
- 8 Spatz, D. R. *et al.* Globally threatened vertebrates on islands with invasive species. *Science Advances* **3**, e1603080, doi:10.1126/sciadv.1603080 (2017).
- 9 Wilson, K. *et al.* Measuring and Incorporating Vulnerability into Conservation Planning. *Environmental Management* **35**, 527-543, doi:10.1007/s00267-004-0095-9 (2005).
- 10 Hansen, M. C. *et al.* High-Resolution Global Maps of 21st-Century Forest Cover Change. *Science* **342**, 850-853, doi:10.1126/science.1244693 (2013).
- 11 Venter, O. *et al.* Sixteen years of change in the global terrestrial human footprint and implications for biodiversity conservation. *Nature communications* **7**, doi:10.1038/ncomms12558 (2016).
- 12 Ellis, E. C. & Ramankutty, N. Putting people in the map: anthropogenic biomes of the world. *Frontiers in Ecology and the Environment* **6**, 439-447, doi:10.1890/070062 (2008).
- 13 Balmford, A. *et al.* Capturing the Many Dimensions of Threat: Comment on Salafsky *et al.* *Conservation Biology* **23**, 482-487, doi:DOI 10.1111/j.1523-1739.2009.01196.x (2009).
- 14 Raiter, K. G., Possingham, H. P., Prober, S. M. & Hobbs, R. J. Under the radar: mitigating enigmatic ecological impacts. *Trends in Ecology & Evolution* **29**, 635-644, doi:<https://doi.org/10.1016/j.tree.2014.09.003> (2014).
- 15 Tulloch, V. J. D. *et al.* Why do we map threats? Linking threat mapping with actions to make better conservation decisions. *Frontiers in Ecology and the Environment* **13**, 91-99, doi:10.1890/140022 (2015).
- 16 Brooks, T. M. *et al.* Harnessing biodiversity and conservation knowledge products to track the Aichi Targets and Sustainable Development Goals. *Biodiversity* **16**, 157-174, doi:10.1080/14888386.2015.1075903 (2015).
- 17 Juffe-Bignoli, D. *et al.* Assessing the Cost of Global Biodiversity and Conservation Knowledge. *PLOS ONE* **11**, e0160640, doi:10.1371/journal.pone.0160640 (2016).
- 18 IUCN. *The IUCN Red List of Threatened Species*, <<http://www.iucnredlist.org>> (2019).

270 19 Salafsky, N. *et al.* A Standard Lexicon for Biodiversity Conservation: Unified Classifications of Threats and
271 Actions. *Conservation Biology* **22**, 897-911, doi:10.1111/j.1523-1739.2008.00937.x (2008).
272 20 BirdLife International. Monitoring Important Bird Areas: a global framework version 1.2. (BirdLife
273 International, Cambridge, UK, 2006).
274 21 Hoffmann, M. *et al.* The Impact of Conservation on the Status of the World's Vertebrates. *Science* **330**, 1503-
275 1509, doi:DOI 10.1126/science.1194442 (2010).
276 22 Hof, C., Araujo, M. B., Jetz, W. & Rahbek, C. Additive threats from pathogens, climate and land-use change
277 for global amphibian diversity. *Nature* **480**, 516-519 (2011).
278 23 Mammides, C. *et al.* Increasing geographic diversity in the international conservation literature: A stalled
279 process? *Biological Conservation* **198**, 78-83, doi:<https://doi.org/10.1016/j.biocon.2016.03.030> (2016).
280 24 Holmes, N. D. *et al.* Globally important islands where eradicating invasive mammals will benefit highly
281 threatened vertebrates. *PLOS ONE* **14**, e0212128, doi:10.1371/journal.pone.0212128 (2019).
282 25 Sanderson, E. W. *et al.* The Human Footprint and the Last of the Wild. *Bioscience* **52**, 891-904,
283 doi:10.1641/0006-3568(2002)052 (2002).
284 26 Secretariat of the Convention on Biological Diversity. 81 + vii (Montreal, 2006).
285 27 Hulme, P. E. Protected land: Threat of invasive species. *Science* **361**, 561-562, doi:10.1126/science.aau3784
286 (2018).
287 28 Watson, J. E. M. *et al.* Protect the last of the wild. *Nature* **563**, 27-30 (2018).
288 29 Mittermeier, R. A. *et al.* Wilderness and biodiversity conservation. *Proceedings of the National Academy of*
289 *Sciences* **100**, 10309-10313, doi:10.1073/pnas.1732458100 (2003).
290 30 Di Marco, M., Ferrier, S., Harwood, T. D., Hoskins, A. J. & Watson, J. E. M. Wilderness areas halve the
291 extinction risk of terrestrial biodiversity. *Nature*, doi:10.1038/s41586-019-1567-7 (2019).
292 31 Barnosky, A. D., Koch, P. L., Feranec, R. S., Wing, S. L. & Shabel, A. B. Assessing the causes of Late
293 Pleistocene extinctions on the continents. *Science* **306**, 70-75, doi:10.1126/science.1101476 (2004).
294 32 Yaculic, C. B., Sanderson, E. W. & Uriarte, M. Anthropogenic and environmental drivers of modern range
295 loss in large mammals. *Proceedings of the National Academy of Sciences* **108**, 4024-4029,
296 doi:10.1073/pnas.1015097108 (2011).
297 33 Butchart, S. H. M. *et al.* Using Red List Indices to measure progress towards the 2010 target and beyond.
298 *Philosophical Transactions of the Royal Society B: Biological Sciences* **360**, 255-268,
299 doi:10.1098/rstb.2004.1583 (2005).
300 34 Rodrigues, A. S. L. *et al.* Spatially Explicit Trends in the Global Conservation Status of Vertebrates. *PLOS*
301 *ONE* **9**, e113934, doi:10.1371/journal.pone.0113934 (2014).
302 35 Di Minin, E. *et al.* Identifying global centers of unsustainable commercial harvesting of species. *Science*
303 *Advances* **5**, eaau2879, doi:10.1126/sciadv.aau2879 (2019).
304 36 Dirzo, R. *et al.* Defaunation in the Anthropocene. *Science* **345**, 401-406, doi:10.1126/science.1251817 (2014).
305 37 Ripple, W. J. *et al.* Bushmeat hunting and extinction risk to the world's mammals. *Royal Society Open Science*
306 **3**, doi:10.1098/rsos.160498 (2016).
307 38 Evans, M. C. *et al.* The Spatial Distribution of Threats to Species in Australia. *BioScience* **61**, 281-289,
308 doi:10.1525/bio.2011.61.4.8 (2011).
309 39 Schipper, J. *et al.* The Status of the World's Land and Marine Mammals: Diversity, Threat, and Knowledge.
310 *Science* **322**, 225-230, doi:10.1126/science.1165115 (2008).
311 40 Redford, K. H. The Empty Forest. *Bioscience* **42**, 412-422 (1992).
312 41 Stokstad, E. The empty forest. *Science* **345**, 396-399, doi:10.1126/science.345.6195.396 (2014).
313 42 McCullough, D. G., Work, T. T., Cavey, J. F., Liebhold, A. M. & Marshall, D. Interceptions of Nonindigenous
314 Plant Pests at US Ports of Entry and Border Crossings Over a 17-year Period. *Biological Invasions* **8**, 611,
315 doi:10.1007/s10530-005-1798-4 (2006).
316 43 Theoharides, K. A. & Dukes, J. S. Plant invasion across space and time: factors affecting nonindigenous
317 species success during four stages of invasion. *The New phytologist* **176**, 256-273, doi:10.1111/j.1469-
318 8137.2007.02207.x (2007).
319 44 Pyšek, P. *et al.* Geographical and taxonomic biases in invasion ecology. *Trends in Ecology & Evolution* **23**,
320 237-244, doi:<https://doi.org/10.1016/j.tree.2008.02.002> (2008).
321 45 Jung, M. *et al.* Areas of global importance for terrestrial biodiversity, carbon, and water. *bioRxiv*,
322 2020.2004.2016.021444, doi:10.1101/2020.04.16.021444 (2020).
323 46 Hulme, P. E. *et al.* Greater Focus Needed on Alien Plant Impacts in Protected Areas. *Conservation Letters* **7**,
324 459-466, doi:10.1111/conl.12061 (2014).
325 47 Lydeard, C. *et al.* The Global Decline of Nonmarine Mollusks. *Bioscience* **54**, 321-330,
326 doi:doi:10.1641/0006-3568(2004)054[0321:TGDONM]2.0.CO;2 (2004).
327 48 McGeoch, M. A. *et al.* Global indicators of biological invasion: species numbers, biodiversity impact and
328 policy responses. *Diversity and Distributions* **16**, 95-108, doi:10.1111/j.1472-4642.2009.00633.x (2010).

- 49 Coad, L. *et al.* Widespread shortfalls in protected area resourcing significantly undermine efforts to conserve biodiversity. *Frontiers in Ecology and the Environment* **17**, 259-264, doi:10.1002/fee.2042 (2019).
- 50 BirdLife International & NatureServe. Bird species distribution maps of the world. BirdLife International, Cambridge, United Kingdom and NatureServe, Arlington, United States. (2017).
- 51 IUCN. Red List of threatened species v 2017.3. (2017).
- 52 IUCN and The Conservation Measures Partnership. IUCN – CMP Threats Classification Scheme, version 3.2. 20 (The International Union for the Conservation of Nature and The Conservation Measures Partnership, Gland, Switzerland, 2019).
- 53 Olson, D. M. *et al.* Terrestrial Ecoregions of the World: A New Map of Life on Earth. *Bioscience* **51**, 933-938, doi:10.1641/0006-3568(2001)051[0933:teotwa]2.0.co;2 (2001).
- 54 Venables, W. N. & Ripley, B. D. *Modern Applied Statistics with S. Fourth Edition.* . (Springer, 2002).

Acknowledgements

We thank the 1000s of people who participate in the red list. We also thank Dr Simon Stuart for valuable input on the amphibian maps. We thank Prof. Nick Dulvy and Dr Simon Stuart for early input on the approach. This work is supported by the Cambridge Conservation Initiative collaborative grants programme (all), EUs Horizon 2020 Marie Skłodowska-Curie action (No 706784, JG), VILLUM FONDEN (VKR023371, JG), KR Foundation and Hempel Foundation (Designing a brighter future for biodiversity) NDB and MBJH.

Author Contributions Statement

JG conceived the study. MBJH and JG designed the study and analysis with substantial input from AJ. MH, SHMB, and CH-T facilitated access to data and provided important context for its use. JG and MBJH led the interpretation of data and writing of the manuscript, with valuable input from AB, NDB, SHMB, MPD, CH, CH-T, MH, NJBI, LLI, AJ, CLO, and PV throughout the process.

Competing Interests Statement

The authors declare no competing interests.

Figure legends

Fig. 1. | Probability of impact for amphibians. Probability that a randomly selected amphibian occurring in a 50x50 km cell is impacted by (a) logging, (b) agriculture, (c) hunting, (d) pollution, (e) invasive species, and (f) climate change. Darker colours indicate higher probability. Zero indicates no species is affected, and one that all species occurring are affected. Grey indicates areas with fewer than 10 species for which the impact probability has not been estimated. (g) shows for each cell the threat with the highest probability of impact and (h) shows the variability of the estimates estimated by resampling threat-classes of each species based on the proportion of Data Deficient species in a given cell (see Methods).

Fig. 2. | Probability of impact for birds. Probability that a randomly selected bird occurring in each 50x50 km cell is impacted by (a) logging, (b) agriculture, (c) hunting, (d) pollution, (e) invasive species, and (f) climate change. Darker colours indicate higher probabilities. Zero indicates no species is affected, and one that all species occurring are affected. Grey indicates areas with fewer than 10 species for which the impact probability has not been estimated. (g) shows for each cell the threat with the highest probability of impact and (h) shows the variability of the estimates estimated by resampling threat-classes of each species based on the proportion of data deficient species in a given cell.

Fig. 3. | Probability of impact for mammals. Probability that a randomly selected mammal occurring in each 50x50 km cell is impacted by (a) logging, (b) agriculture, (c) hunting, (d) pollution, (e) invasive species, and (f) climate change. Darker colours indicate higher probability. Zero indicates no species is affected, and one that all species occurring are affected. Grey indicates areas with fewer than 10 species for which the impact probability has not been estimated. (g): shows for each cell the threat with the highest probability of impact and (h) shows the variability of the estimates estimated by resampling threat-classes of each species based on the proportion of data deficient species in a given cell.

Fig. 4. | Global hotspots of threat. Global threat hotspots (90th percentile of risk, the product of the probability of impact and the species richness) for amphibians, birds and mammals for the six principal threats: (a) agriculture, (b) hunting and trapping, (c) logging (d) pollution (e) invasive species and diseases, and (f) climate change. Colours indicate whether an area falls within a threat hotspot for one or more taxon groups. g: shows the relative importance of each pixel across species and threats. It is the count of the number of times a pixel falls into a hotspot region for any taxon or threat, so pixels with higher values indicate that it falls in the 90th percentile for many taxonomic groups and threats.

Fig. 5. | Comparison between probability of impact and pressure. Relationship between the Human Footprint (HF) and the probability of threats estimated from the Red List for amphibians, birds and mammals for land use (a), and for two threats for which the HFI does not explicitly include: hunting and trapping (b) and climate change (c). Grey lines indicate a 1:1 linear relationship. (d-f) show residuals from unity. Negative values (red colours) indicate where the standardised HFI is higher than our estimated probability of threat occurrence, P_{Th} and, conversely, positive values (blue colours) indicate where P_{Th} is higher than the standardised HFI value.

Methods

Species level data

Species range maps were derived from BirdLife International & NatureServe⁵⁰ and IUCN⁵¹. Threat data were from the IUCN Threats Classification Scheme (Version 3.2) which contains 11 primary threat classes and almost 50 sub-classes⁵². In Red List assessments, assessors assign those threats that impact the species. For birds, the scope of the impact is also recorded categorically as the percentage of the species population which the threat impacts (unknown, negligible, <50% 50-90% or >90%) and the severity, describing the scale of the impact on population declines: unknown, no decline, negligible declines, fluctuations, slow but significant declines (<20% over 10 years or three generations), rapid declines (20-30%), very rapid declines (>30%).

Model development approach

We designed our analytical framework with three considerations in mind. Firstly, the threat location information is limited: for each species the data only describe whether a species is threatened by a given activity anywhere within its range (data on the timing, scope and severity of threats are available only for birds and are not spatially explicit). Second, we wanted to compare the spatial patterns of threat against independent data on spatial distributions of human activities. Third, for many activities the relationship between human activity (e.g. hunting or invasive species & diseases) and biodiversity response is poorly

understood. We therefore chose not to incorporate known patterns of human activity as explanatory variables in our models.

In the absence of global datasets on the spatial patterns of probability or impact of each threat, we used a simulation approach to develop our models and assess the ability of different model-parameterizations to reproduce our simulated threat. This process had four steps (Extended Data Figure 1).

Simulated threat intensity maps: First, we simulated a continuous synthetic threat across sub-Saharan Africa. The concept behind this is that a credible model should be able to reproduce a “true”, synthetic threat pattern based on information comparable to that available in the Red List. To test this, we generated a set of synthetic, continuous surfaces of threat intensity with different levels of spatial autocorrelation and random variation (Supplementary Figure 1). This was achieved by taking a grid of 50×50 km ($2,500 \text{ km}^2$) pixels across the Afrotropic biogeographic realm (i.e Sub-Saharan Africa). Threat intensity was modelled as a vector of random variables, Z , one for each pixel i , generated with correlation structure given by the distance matrix between points weighted by a scalar value, r , indicating the degree of correlation (Eq. S1 – S3). Four values of r were used, 1×10^{-6} which yields very strong autocorrelation, 1×10^{-4} which yields strong autocorrelation, 0.05, which yields moderate autocorrelation and 0.3, which produces a low-correlation, localised pattern (Supplementary Figure 1).

$$Z(r) = U^T \text{Norm}(n, 0, 1) \quad \text{Eq. S1}$$

$$W = UU^* \quad \text{Eq. S2}$$

$$W = e^{(-rD)} \quad \text{Eq. S3}$$

Where r is a scalar determining the degree of spatial autocorrelation, as r decreases the autocorrelation increases; D is the Euclidean distance matrix between each pair of pixels; W is the matrix of weights for the threat intensity; U and U^* are the upper triangular factor of the Choleski decomposition of W and its conjugate transpose; U^T is the transpose of U ; and n is the number of pixels.

We chose the Afrotropic biogeographic realm (e.g. Sub-Saharan Africa) as our geography within which to develop the modelling approach because it permitted more rapid iterations than a global scale simulation whilst also retaining characteristics of importance for the model evaluation such as strong environmental gradients and heterogeneity in species richness. However, for the simulation, no information from the geography or overlapping species ranges are used, except the spatial configuration of the polygons. Thus, the use of the Afrotropic is purely to avoid generating thousands of complex geometries for the purpose of the simulation. Using a real geography and actual species ranges ensures that our simulation contains conditions that are observed in reality (e.g. areas of high and low species richness also observed in the real world). We took the simulated threat maps generated through this process to be our “true” likelihood of a

randomly drawn species occurring in that location being impacted by the synthetic threat (Supplementary Figure 1).

Simulating Red Listing process: Second, we wanted to simulate the red listing process whereby experts evaluate whether a threat is impacting a species based on the overall threat intensity within its range. For this, we used the range maps for all mammal species within Africa and assigned a binary threat classification (i.e. affected or not affected) to each species based on the values of the synthetic threat within each species' range. We assumed that the binary assessment of threat for a species is based on whether the level of impact across a proportion of its range is judged as significant. This step was intended to replicate the real red-listing process, where assessors define threats that impact the species based on an assessment of the information available on threatening mechanisms and species responses. In practice, this was done by overlaying the real range maps for mammals over the four simulated threat surfaces and assessing the intensity of synthetic threat within each species range map. We wanted to assign species impacts considering that species will be more likely to be impacted if a greater part of their range has high threat intensity. Understanding how to set a threshold for what intensity would constitute sufficient threat to be assessed as affected is a complicated exercise. Thus, we tested three different thresholds to capture different assumptions. These thresholds were chosen following discussion with leading experts on the red-listing process. More specifically we calculated the 25th, 50th and 75th percentile of threat intensity across pixels within the species range. We then used a stochastic test to convert these quantiles to binary threat class, *C*. For each species we produced a set of 10 draws from a uniform distribution bounded by 0 and 1. If over half of the draws were lower than the threat intensity quantile, then species was classified as threatened for that percentile.

The above simulation assumes perfect knowledge of the threat intensities across the species range which might not always be the case in the actual red-listing process. In real life, certain areas within species ranges are less well known for a suite of different reasons. To incorporate some uncertainty about the knowledge of the red-listing experts about the “true” threat intensity, we constructed a layer to describe the spatial data uncertainty associated with the Red List. This aspect was intended to simulate the imperfect knowledge of the simulated ‘Red List assessors’. This layer was calculated as the proportion of species present in a given location that are categorised as Data Deficient, in other words there is insufficient information known about the species to assess its extinction risk using the IUCN Red List Criteria (Extended Data Figure 7). Then when calculating the 25th, 50th and 75th percentile of threat intensity across each range, we weighted this calculation by one minus the proportion of Data Deficient species, so that more uncertain places (those with a greater proportion of Data Deficient species) contributed less to the calculation than threat intensities in locations where knowledge was more certain. These were then converted to a binary threat class accounting

for uncertainty in expert knowledge amongst the simulated ‘assessors’, $C_{Uncertain}$, using the same stochastic process described above for the calculation of C .

This step produced, for each species, a threat classification analogous to the threat classification assigned by experts as part of the IUCN Red List process. Six sets of threat classifications were produced for each synthetic threat surface, based on 25th, 50th and 75th percentile with perfect ($C_{0.25}$, $C_{0.5}$, $C_{0.75}$) or uncertain ($C_{Uncertain-0.25}$, $C_{Uncertain-0.5}$, $C_{Uncertain-0.75}$) spatial knowledge.

Model formulation and selection: Third, using all species polygons with assigned threat assessment from step 2 (i.e. affected or not affected) we fitted nine candidate models and predicted for each grid cell the estimated probability of impact. Then in a fourth step, the predicted probabilities of impact produced in step 3 were compared with the original synthetic threat maps created in step 1 to test the predictive ability our models.

The Red List threat assessment does not contain information on where within the range the impact occurs. Therefore, a species with a very small range provides higher spatial precision about the location of the impact, whereas a species with a large range may be impacted anywhere within a wide region. To address this lack of precision in the impact location, we took the area of each species range, (i.e. the range size, ‘ R ’) to serve as a proxy for the spatial certainty of the impact information. The certainty that a species was impacted or not impacted in a given cell depended on its range size, R . The models we evaluated therefore incorporated the range (R) in different ways (Supplementary Table 1).

Models were fitted as a binomial regression with logit link function. For each pixel, the model predicts the ‘probability of impact’, P_{Th} , in other words the probability that if you sampled a species at random from those that occur in that pixel, the species would be impacted by the activity being considered. To account for uncertainties in the simulation of the threat assessment process (thresholds for impact, perfect or imperfect knowledge) models were fitted to the six sets of threat codes ($C_{0.25}$, $C_{0.5}$, $C_{0.75}$, $C_{Uncertain-0.25}$, $C_{Uncertain-0.5}$, $C_{Uncertain-0.75}$) and the root mean squared error (RMSE) calculated between P_{Th} (estimated impact probability) and the simulated threat intensity, $Z(r)$, for each value of correlation structure, r . For each simulation we ranked the different models according to their model fit measured by RMSE. We assessed these ranks across all simulations and sets of threat codes. We evaluated models based on the ranks of RMSE, across the threat code sets and threat intensity maps. Rank distributions for each model are shown in Extended Data Figure 2 and results from these models are shown in Supplementary Table 1 and 2.

All models were correlated (Pearson's $r^2 > 0.5$) albeit with some variation between model types and across the simulation parameters (Supplementary Figure 2). However, some models had greater predictive accuracy when evaluated using RMSE. The top four ranking models were, in order of decreasing summed rank, (1) inverse of cube root range size as a weight, (2) inverse 2.5 root range size as a weight, (3) inverse square root range size as a weight and (4) inverse natural logarithm of range size as a weight. The fact that these four models show good model fit suggests that the best model structure has a measure of range size as a weight, but that the model was not particularly sensitive to the transformation of range size.

The best-fitting model across the range of simulations parameters was an intercept only logistic regression where the response variable was the binary threat code (1 = threatened, 0 = not threatened) for each species in the pixel and using the inverse cube root of the range size of each species as a weighting. The model was concordant across the set of simulated datasets with a relationship that was predominantly linear with r^2 between 0.47 and 0.7, depending on simulation parameters for $Z(r)$ in 0.05, 10^{-4} and 10^{-6} , centred around unity, and with root mean squared error ranging between 0.129 – 0.337 depending on simulation parameters (Figures S2 and S3). The choice of the inverse cube root range size weight was based on the performance of this against eight other model types (Supplementary Figure 4 Supplementary Table 1).

A decomposition of variance in model performance, using a binomial regression model, with RMSE as the dependent variable and model type, knowledge level and autocorrelation structure as the independent factorial variables, showed that knowledge about the threats underlying each species range and how that threat information is used in assessment, explained the vast majority (94.7%) of the variation in RMSE outcomes (Supplementary Figure 4).

For birds, further information on the scope of the threat was available as an ordinal variable describing the fraction of range that the threat covers. We explored the use of scope in our models but concluded that to avoid arbitrary decisions about the scope of non-threatened species (where they are either not threatened anywhere or threatened in only a small part of their range), and for consistency with other taxonomic groups, we would model birds using the same model structure as used for mammals and amphibians (see supplementary methods for further details).

Mapping probability of impact

Once the best performing model was identified using the simulated data, we then used this model on the actual Red List threats and range data to develop of threat maps. This model produced threat maps for each taxonomic group (amphibians, birds, mammals) of the probability of impact, P_{Th} , for each individual threat. This estimates for a given pixel, threat and taxonomic group the probability that a randomly sampled species

with a range overlapping with that pixel is being impacted by the threat, while taking into account spatial imprecision in the Red List data.

Threat maps were generated using range map data and threat assessments from the IUCN Red List¹⁸. We intersected range maps for 22,898 extant terrestrial amphibians (n = 6,458), birds (n = 10,928; excluding the spatial areas within the range that are associated with “Passage” – where the species is known or thought very likely to occur regularly during a relatively short period(s) of the year on migration) and mammals (n = 5,512; including those with uncertain ranges) with a global 50x50 km (2,500 km²) resolution, equal area grid for the terrestrial world. This provided, for each 50x50 km pixel, a list of the species whose range overlapped it, along with the associated range size of each species. For each pixel and taxonomic group (amphibians, birds and mammals) independently, we then modelled the ‘probability of impact’, $P_{Th,Activity}$, (e.g. $P_{Th,Logging}$ for logging, $P_{Th,Agriculture}$ for agriculture or $P_{Th,Pollution}$ for pollution) for each of the six threats: agriculture, hunting & trapping, logging, pollution, invasive species & diseases, and climate change. We focused on these as the six main threats as defined by IPBES⁴, but our methodological framework is flexible and could be expanded to other threats in the IUCN classification¹⁹. We used only taxonomic groups with a sufficiently high total number of species and where they have been comprehensively assessed so that potential biases associated with the groups of species prioritized by experts are avoided.

Calculating uncertainties for the threat probability: We estimated a measure of uncertainty associated with our impact probability predictions using maps of the proportions of Data Deficient species in each cell within each taxonomic class (amphibians, birds or mammals) as a measure of knowledge-certainty in that cell. The rationale for this approach is that places with more Data Deficient species with unknown threatened status, should have greater uncertainty in the probability of impact. Therefore, we created greater variation in the data where there were more Data Deficient species. We used the knowledge-certainty map to probabilistically draw a sample of 100 threat codes for each species, based on the median Data Deficiency across the species range. The random sample changed the species threat code with a probability related to the proportion of Data Deficient species within its range. If the median proportion of data deficient was zero, then we assumed that there was a small probability (0.005) that the species could have been incorrectly coded. Where the median proportion was greater than zero, the probability increased linearly. So, for a species with 5% Data Deficient species within its range, the sample changed the species threat code with a probability close to 5%, or, if the median proportion was equal to 0.5, then the probability of the species being incorrectly assigned was equal to 0.5. We then fitted the impact probability model with each of the 100 species threat codes and generated a distribution of predicted threat probabilities in each grid cell, from which we took the 95% confidence intervals as the uncertainty estimate (Extended Data Figures 8-10).

Evaluating modelled threat patterns

We evaluated the spatial patterns of threat based on the real Red List threat assessment data against empirical data in two independent ways. First we compared the probability of impact from logging and agriculture combined within forested biomes (i.e. corresponding to remotely detected forest loss, which we refer to the probability of impact from forest loss, $P_{Th, forest-loss}$) to data on forest cover change¹⁰. Forest cover change was aggregated from their native 30x30 m (900 m²) resolution pixels to our 50x50 km resolution pixels using Google Earth Engine. For each 50x50 km pixel we calculated the total area lost between 2000 and 2013 and the area lost as a proportion of the area in 2000. We restricted our analysis to forested biomes: a) Tropical and subtropical moist broadleaf forests, b) Tropical and subtropical dry broadleaf forests, c) Tropical and subtropical coniferous forests, d) Temperate broadleaf and mixed forests, e) Temperate Coniferous Forest and f) Boreal forests / Taiga, following WWFs ecoregions classification⁵³. The relationship between forest loss and the probability of impact from forest loss as captured by agriculture and logging overall showed a significant positive correlation, $P_{Th, forest-loss}$ increased with increasing forest cover loss ($p < 1 \times 10^{-5}$, Supplementary Figure 5) but also showed some nuances.

Second, we evaluated threat levels against threat for ca. 6,000 KBAs assessed by specialists through a rigorously tested and standardized approach developed by Bird Life International²⁰. For a given activity, we calculated the median of predicted impact probabilities within each KBA and then grouped these KBA estimates by KBA severity class. On average, P_{Th} was higher in KBAs assessed as having a high severity of threat from an activity than in KBAs classed as having low threat. Significant relationships ($p < 0.05$, Wilcoxon test) were found in one or more taxonomic group for logging, agriculture, hunting and climate change. For both evaluations, we conclude that the modelled spatial patterns of threat were consistent with expectations from the empirical data (Figures S5 – S11). We subsequently shared threat maps with taxon-specific experts from the Red List assessment groups, who qualitatively reviewed the patterns and assessed them as consistent with expert knowledge. Further details on the evaluation methods can be found in the supplementary methods text.

We suggest that the broad concordance with empirical data in two independent evaluations demonstrates that the maps of impact probability are sufficiently plausible to underpin the findings of this study. We provide a framework that can easily be updated with future versions of the IUCN data, and we also stress that our approach should be viewed as an initial attempt to map patterns of threat impacts, which should be used iteratively to guide collection of new data and improvement of the mapping approaches used.

Comparing threat occurrence likelihoods and human footprint index

Human Footprint Index (HFI) data for the year 2009 was taken from Venter, et al.¹¹. The native resolution of the index was 1 km² so we calculated the mean HFI in each 50x50 km pixel used in our analysis. The HFI was standardised to lie within the bounds 0 and 1 by dividing by the maximum HFI index value (50).

We compared the standardised, averaged HFI values to the predicted likelihood of threat occurring from land use change, hunting and trapping and climate change. For land use change we combined agriculture and logging. Hence, for land use change we calculated the unweighted mean threat occurrence likelihood across taxa for logging and agriculture. For hunting we took the mean threat occurrence likelihood across taxa, whilst for climate change we used the predicted threat occurrence likelihood for birds.

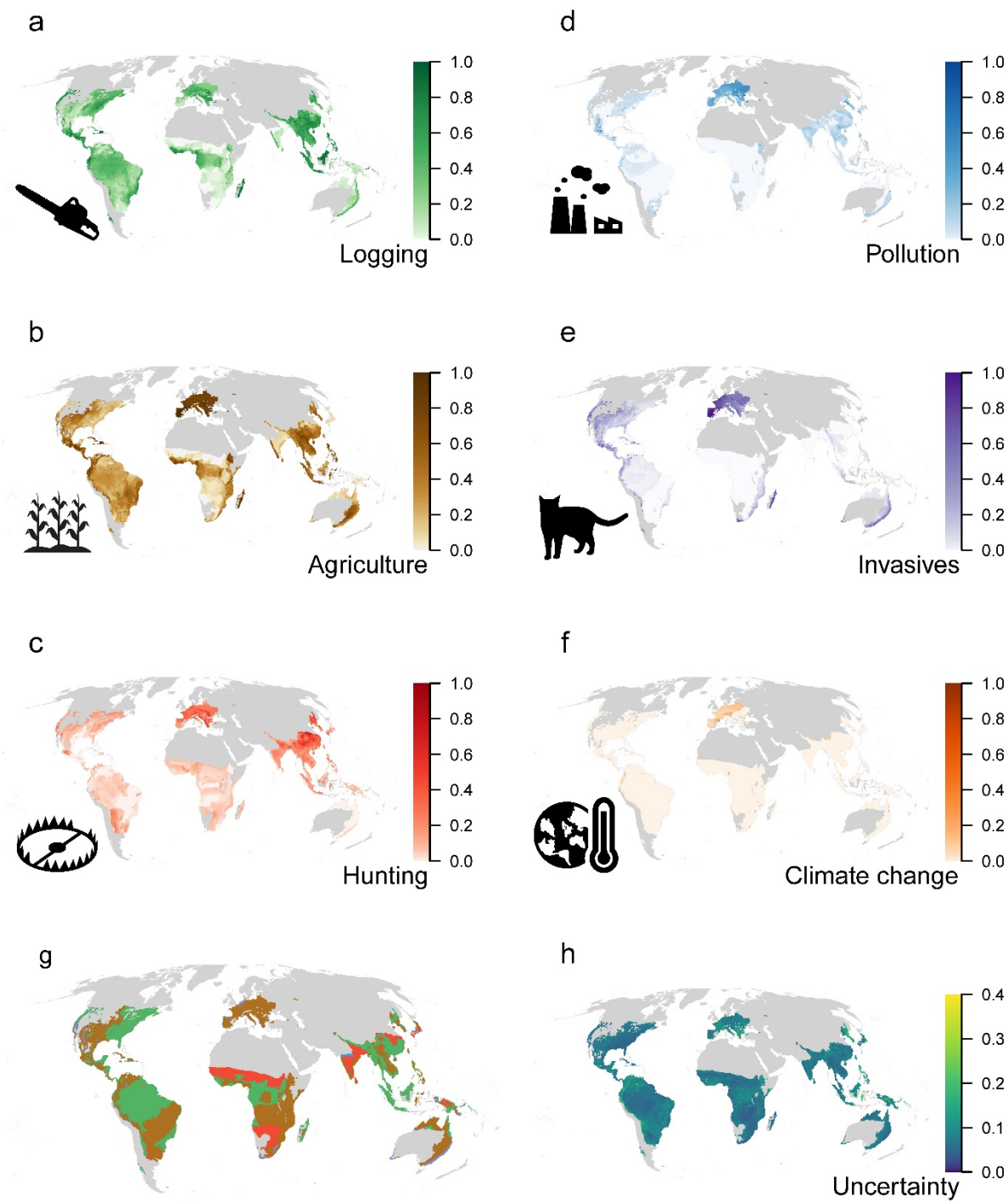
To plot the spatial relationship between HFI and mean threat occurrence likelihood we used a 2-dimensional kernel density estimator (MASS package⁵⁴ to estimate the variation in density of pixels for a given HFI and mean threat occurrence likelihood.

Data availability

Data on range maps are freely available at <https://www.iucnredlist.org/resources/spatial-data-download> and <http://datazone.birdlife.org/species/requestdis>. IUCN threat classification assessment data can be downloaded using the Red List API (<http://apiv3.iucnredlist.org/api/v3/docs>) or on request from IUCN's Global Species Programme Red List Unit (redlist@iucn.org). Other data are freely available using citations in the manuscript.

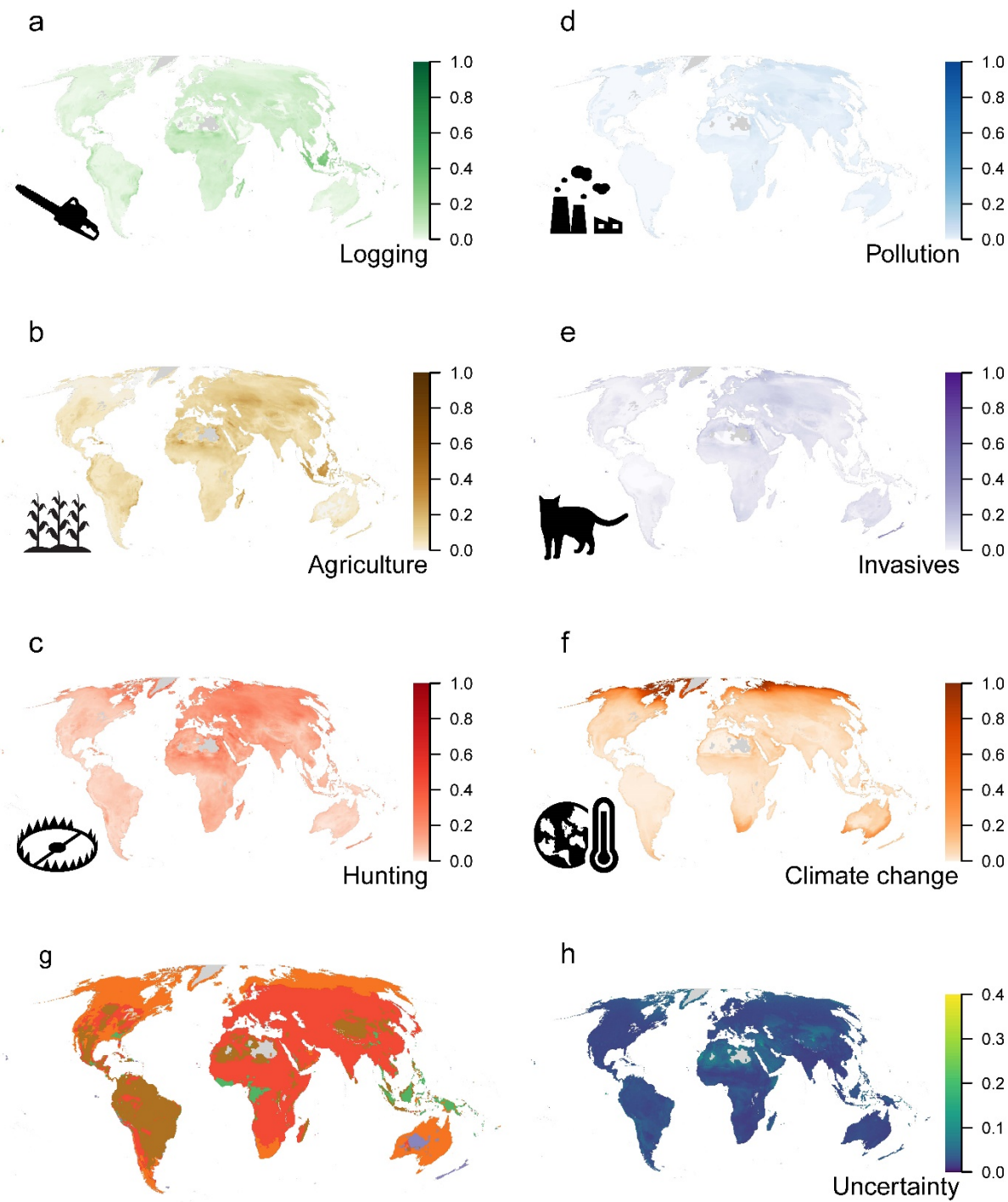
Code Availability

Code is available from the github repository <https://github.com/mikeharfoot/ThreatMapping>

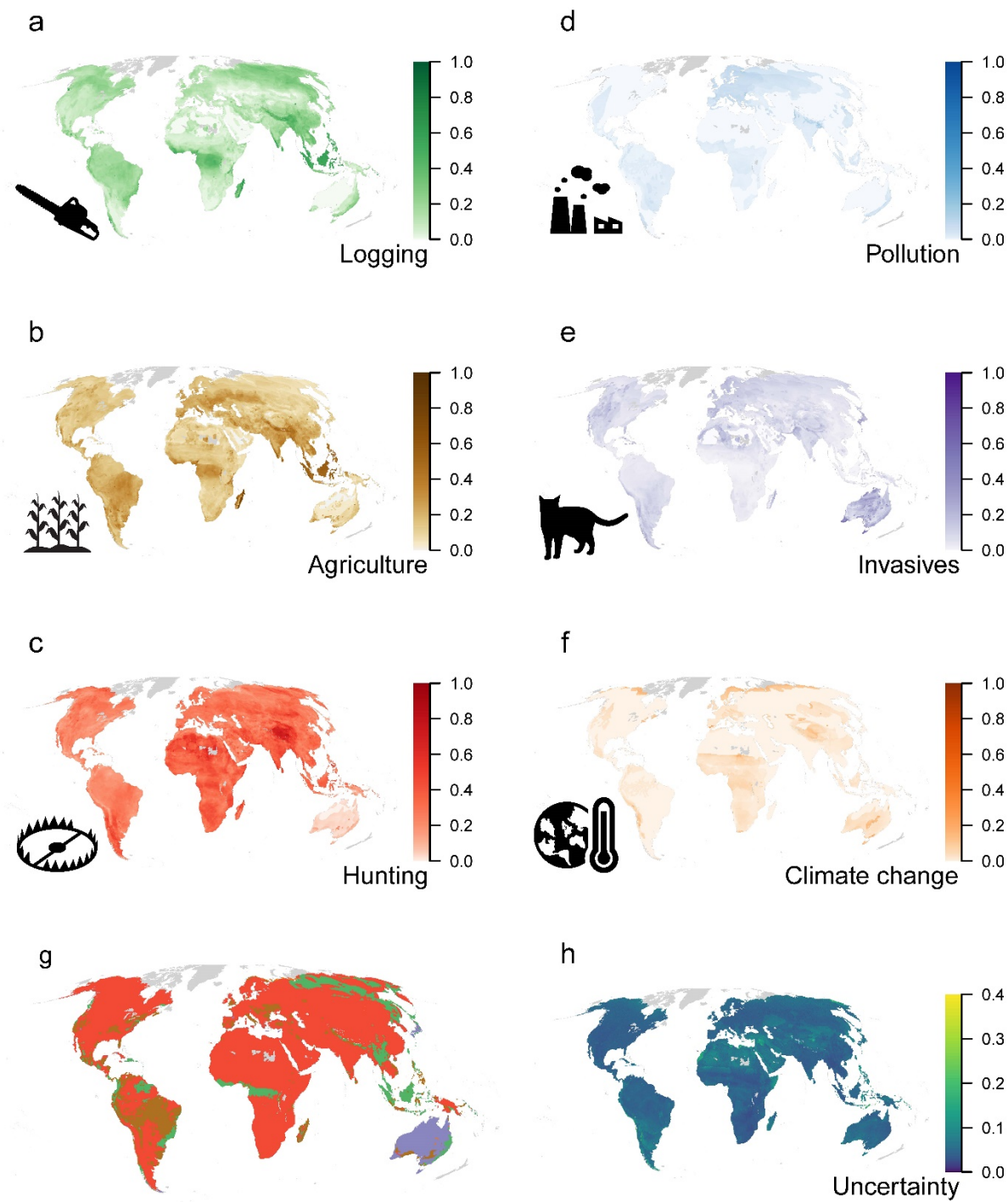


644

645



647
648



650
651

